J. Chem. Sci. Vol. 129, No. 4, April 2017, pp. 441–448. © Indian Academy of Sciences.
DOI 10.1007/s12039-017-1261-y

REGULAR ARTICLE

Synthesis, thermal properties and photoisomerization of *trans*-$[Ru(NO)Py_2Cl_2(H_2O)]H_2PO_4{\cdot}H_2O$

ALEXANDER N MAKHINYA[a,b,*], ILYA V KOROLKOV[a,b], MAXIM A IL'IN[a,b], IRAIDA A BAIDINA[a], PAVEL E PLUSNIN[a,b], EUGENI A MAXIMOVSKI[a,b], ELIZAVETA A BELETSKAYA[a,b] and NINA I ALFEROVA[a]

[a]Nikolaev Institute of Inorganic Chemistry, Siberian Branch of Russian Academy of Sciences, 3 Akad. Lavrentiev Ave., Novosibirsk 630090, Russia
[b]Novosibirsk State University, 1 Pirogova Str., Novosibirsk 630090, Russia
Email: sas.fen@mail.ru; decanat@fen.nsu.ru; niic@niic.nsc.ru

MS received 7 December 2016; revised 1 March 2017; accepted 5 March 2017

Abstract. The reaction of *trans*-$[Ru(NO)Py_2Cl_2(OH)]$ with concentrated o-phosphoric acid, after washing the mixture with diethyl ether, gave *trans*-$[Ru(NO)Py_2Cl_2(H_2O)]H_2PO_4{\cdot}2H_3PO_4{\cdot}H_2O$ (**I**) in nearly quantitative yield. The structure of this compound was determined by X-ray diffraction analysis: space group P-1. Washing of **I** with ethanol afforded the dihydrophosphate salt *trans*-$[Ru(NO)Py_2Cl_2(H_2O)]H_2PO_4{\cdot}H_2O$ (**II**) (yield 97%). The thermal decomposition of **I** and **II** in a helium atmosphere resulted in the formation of ruthenium phosphide RuP as a predominant component along with Ru_2P or RuP_2. Preliminary photoisomerization experiments for *trans*-$[Ru(NO)Py_2Cl_2(OH)]$ and *trans*-$[Ru(NO)Py_2Cl_2(H_2O)]H_2PO_4{\cdot}H_2O$ suggested the presence of metastable states. DSC experiments have been carried out for both compounds. The measured kinetic parameters for the metastable decay for *trans*-$[Ru(NO)Py_2Cl_2(H_2O)]H_2PO_4{\cdot}H_2O$ were $E_a = 90.7 \pm 2.4$ kJ/mol, $\log_{10}(k_0/sec^{-1}) = 18.9 \pm 0.6$, and $T_d = 217$ K.

Keywords. Ruthenium nitrosyl complexes; pyridine; X-ray crystallography-thermal analysis; photoinduced linkage isomer; ruthenium phosphide; DSC.

1. Introduction

Ruthenium phosphides RuP and Ru_2P are known as stable catalysts for electrochemical oxygen reduction, seem to be good candidates as substrate in fuel cell electrodes[1] and more active catalysts than Ru for the hydrodesulfurization of dibenzothiophene and hydrodenitrogenation of quinoline.[2] Phosphorus-rich phosphides, for example, – RuP_2 and RuP_3, are n-type semiconductors with band gaps of 0.8 eV[3] and 1.67 eV,[4] respectively. The convenient method for synthesis is heating of a mixture of elements at 1200°C (RuP_2) and 1000°C (RuP_3). Catalytically active phosphides Ru_2P and RuP can be prepared by mixing of $RuCl_3$ and hypophosphite solutions and heating of the resulting precipitate in inert atmosphere at ~550°C.[1,2] And the other process of preparation of RuP consists of high temperature reduction of pyrophosphate salt, $RuP_2O_7{\cdot}H_2O$ by hydrogen at 800–1000°C.[5] This work shows the new method for synthesis of nanosized particles of RuP by thermolysis of hydrophosphate complex salt of nitrosyl ruthenium.

In the stable state, the NO group is coordinated to the transition metal through the N atom. Exposure of the starting nitrosyl complex to laser radiation produces isomers in which NO is coordinated through either the O atom (MS1 state) or simultaneously the O and N atoms (MS2).[6] Reversible photoisomerization offers scope for the synthesis of hybrid materials combining lattice photochromism, conductance, magnetism, special optical properties, etc in the same crystal.[7–9]

Trans-$[Ru(NO)(Py)_4Cl](PF_6)_2{\cdot}0.5H_2O$[10] and *trans*-$[Ru(NO)Py_2(NO_2)_2(OH)]$[11] exhibit highest known populations of the metastable states among ruthenium nitrosyl complexes and the metastable state (MS1) of *trans*-$[Ru(NO)(NH_3)_4(H_2O)]Cl_3$ has the highest decomposition temperature, $T_d = 293$ K.[6] Thus, we have the interesting combination of pyridine and water molecules in coordination sphere of nitrosyl complex, and hence a high value of T_d may be observed. The purpose of this work is to report the preparation of novel complex salt of dipyridine nitrosylruthenium, its structural investigation, thermal decomposition and preliminary photoisomerization studies.

*For correspondence

2. Experimental

2.1 *Materials and methods*

Trans-[Ru(NO)Py_2Cl_2(OH)] was prepared from K_2[Ru(NO)Cl_5].[12] The latter compound was obtained with an yield of ∼97% from commercially available ruthenium trichloride hydrate as described in the literature.[13] Other reagents and solvents were used as purchased and were reagent grade or better.

Elemental analyses were performed on a EURO EA3000 (Euro Vector). Inductively coupled plasma mass spectrometry (ICP-MS) was performed on "Thermo Scientific", iCAP-6500. Thermal analyses were carried out on thermobalance TG 209 F1 Iris® by NETZSCH (heating rate 10°C/min, He-flow 30 mL/min, Al_2O_3-crucible, sample mass ∼10 mg). Scanning electron microscopy was performed on JEOL JSM 6700F. Energy of the incident beam was 15 keV, working distance – 8 mm. For obtaining picture was used as secondary electron detector, as backscattered electron detector in mode "compo".

2.1a *IR spectra*: IR spectra of the samples were measured in KBr pellets on a Scimitar FTS 2000 FT-IR spectrometer within the wavenumber range 4000–375 cm^{-1}. To detect the formation of photoinduced isomer, the pellets of substance in KBr was irradiated with a diode laser (450 nm, 100 mW) for 30 min while cooling with liquid nitrogen and then the IR spectrum was recorded immediately.

2.1b *X-ray diffraction*: Powder X-ray diffraction examination of ground crystals was performed on Shimadzu XRD-7000 diffractometer (CuK-α radiation, Ni – filter, 2θ range: 5–60°). A polycrystalline sample was slightly ground with hexane in an agate mortar, and the resulting suspension was deposited on the polished side of a standard quartz sample holder, and a smooth thin layer was formed after drying. Indexing of the diffraction patterns was carried out using data for compounds reported in the PDF database (RuP - PDF 010-74-6496, Ru_2P and RuP_2 - PDF 010-89-3031).[14] The range of coherent scattering values for individual peaks was calculated by Scherrer equation with external etalon (Si) band width considering.

2.1c *Single-crystal structure analysis*: Unit cell parameters and intensity data were measured on an automated four-circle X8 APEX Bruker diffractometer (MoKα radiation, graphite monochromator, CCD area detector). The structures were solved by the heavy atom method and refined in the anisotropic approximation; hydrogen atoms were put in idealized positions and refined isotropically. All calculations were performed using SHELXTL.[15] Crystal data and selected refinement details for **I** are given in Table 1. CCDC No.1476880 contains the supplementary crystallographic data for this paper. The copy of *CIF*-file in text-format is shown in Supplementary Information of this paper.

Table 1. X-ray experimental details for *trans*-[Ru(NO)$Py_2Cl_2(H_2O)$]H_2PO_4·$2H_3PO_4$·H_2O (**I**).

Empirical formula	$C_5H_{11}ClN_{1.50}O_{7.50}P_{1.50}Ru_{0.50}$	
Formula weight	344.59	
Crystal system	Triclinic	
Temperature, K	296(2)	
Cell parameters	a = 8.6966(10) Å	α = 91.175
	b = 10.0364(13) Å	β = 103.567
	c = 14.2779(19) Å	γ = 90.160
Space group	P-1	
Z	4	
V, Å^3	1211.1(2)	
ρ_{calc}, g/cm^3	1.890	
μ, mm^{-1}	1.140	
F(000)	692	
Range, ° 2θ	2.41–30.78	
Range h, k, l	$-12 \le h \le 12$	
	$-14 \le k \le 14$	
	$-20 \le l \le 20$	
Measured reflections	25982	
Unique reflections	7482	
[R(int)]	0.0467	
Record area, ° 2θ	25.25	
Completeness of data collection, %	99.9	
Refinement method	Full-matrix LSM against F^2	
Number of parameters refined	365	
Goodness-of-fit (S factor against F^2)	0.994	
R1 [$I > 2\sigma(I)$]	0.0324	
wR2 [$I > 2\sigma(I)$]	0.0653	
R1 (all data)	0.0507	
wR2 (all data)	0.0695	

2.1d *Differential scanning calorimetry*: A NETZSCH DSC 204 F1 Phoenix differential scanning calorimeter was used to study the kinetics and thermal effects of the reversible photoinduced transition. To study MS1 the sample was placed in liquid nitrogen vapor and irradiated with a diode laser (100 mW, 450 nm) for 30 min. The sample was then quickly transferred to a device for DSC. The calorimetric measurements of powdered samples (1–3 mg) were performed in open aluminium crucibles by the heat-flow measurement method at different heating rates of 5.9, 6.0 and 8.9 K/min in a 25 mL/min Ar flow. To increase the accuracy, the measurements were performed without a supply of gas or liquid nitrogen in the measurement cell during the experiment. The sensitivity calibration of the sample carrier sensors and temperature scale were performed by heating and observing crystal-to-crystal transition measurements of standard samples (C_6H_{12}, Hg, KNO_3, In). The processing of the experimental data was performed with the Netzsch Proteus Analysis software.

2.2 *Synthesis of the complexes*

2.2a *Synthesis of trans-[Ru(NO)(Py)$_2$Cl$_2$(H$_2$O)]H$_2$PO$_4$·2H$_3$PO$_4$·H$_2$O (**I**)*: 0.3 g ($7.9\cdot10^{-4}$ mol) of *trans*-[Ru(NO)$Py_2Cl_2(OH)$] was moisturized by 0.5 mL of concentrated *o*-phosphoric acid on porous glass filter; then, the resulting wine-reddish mixture was washed thrice with 5–10 mL diethyl ether and dried in air flow. Yield is 0.51 g (∼96%). Red crystals suitable for a single-crystal X-ray analysis were obtained by the slow evaporation of solution in dilute phosphoric acid. All reactions were conducted at room temperature. Found, %: C–18.2; H–3.3; N–6.4. Anal. calc. for $C_{10}H_{22}N_3O_{15}P_3Cl_2Ru$, %: C–18.3; H–3.1; N–6.4.

2.2b *Synthesis of trans-[Ru(NO)(Py)$_2$Cl$_2$(H$_2$O)]H$_2$PO$_4$·H$_2$O (II)*: 0.3 g ($4.5\cdot10^{-4}$ mol) of *trans*-[Ru(NO)(Py)$_2$Cl$_2$(H$_2$O)]$H_2PO_4\cdot2H_3PO_4\cdot H_2O$ was washed on porous glass filter with 3 mL of ethanol, diethyl ether and dried. Yield is 0.21 g (∼97%). Found, %: C–24.4; H–2.9; N–8.4. Anal. calc. for $C_{10}H_{16}N_3O_7PCl_2Ru$, %: C–24.4; H–3.3; N–8.5.

3. Results and Discussion

3.1 *Synthesis and characterization*

Room-temperature reaction of hydroxo complex *trans*-[Ru(NO)$Py_2Cl_2(OH)$] with concentrated HCl or H_2SO_4 results in protonation of the coordinated hydroxide ion, yielding the corresponding salts of aqua complexes *trans*-[Ru(NO)(Py)$_2$Cl$_2$(H$_2$O)]Cl·2H$_2$O and *trans*-[Ru(NO)(Py)$_2$Cl$_2$(H$_2$O)]HSO_4.[12] Reaction with *o*-H_3PO_4 yields the same aqua complex *trans*-[Ru(NO)(Py)$_2$Cl$_2$(H$_2$O)]$H_2PO_4\cdot2H_3PO_4\cdot H_2O$ (**I**) containing two molecules of *ortho*-phosphoric acid. Washing with ethanol results in removing of acid molecules and formation of *trans*-[Ru(NO)(Py)$_2$Cl$_2$(H$_2$O)]$H_2PO_4\cdot H_2O$ (**II**). Synthesized product contains water molecule indicated by elemental analysis and IR studies. The stretching vibration bands of ν(NO) were observed at 1904 cm^{-1} (**I**) and 1902 cm^{-1} (**II**), and these values fall within a range characteristic of most nitrosyl complexes of ruthenium that combine the diamagnetic metal center Ru(II) and the linearly coordinated species NO^+.[12,16-18] Note that the ν(NO) frequency depends on the ligand that is *trans*- to the nitrosyl group and is shifted to the shorter wavelengths when moving from the neutral hydroxo complex *trans*-[Ru(NO)$Py_2Cl_2(OH)$] (1817 cm^{-1}) to the cationic aqua complex *trans*-[Ru(NO)(Py)$_2$Cl$_2$(H$_2$O)]$^+$ (1897–1904 cm^{-1}).[12,16]

IR-spectra of **I** (ν, cm^{-1}): 3550 m $\nu(OH_{H3PO4})$, 3350 m $\nu(H_2O)$; 3150–3030 weak ν(CH); 2800 wide s $\nu(H_2O_{coord.})$; 2340 wide s ν(OH...O); 1904 *vs* ν(NO); 1636 wide m $\delta(H_2O)$; 1608 m, 1489 weak, 1453 m, 1362 weak ν(C−C), ν(C−N); 1220, 1170 wide s, 988 wide *vs* $\nu(H_2PO_4, H_3PO_4)$; 1221, 1111 weak, 1072 m, 1038, 1016 weak $\delta(CH_{plane})$; 903, 872 weak sh δ(RuOH); 761, 691 s, 651 m $\delta(CH_{out-of-plane})$; 615, 596 weak $\nu(Ru-N_{NO})$, δ(RuNO); 551 ν(Ru−O); 505 s, 495 s sh, 409 m $\delta(H_2PO_4, H_3PO_4)$; 453 m $\nu(Ru-N_{Py})$.

In the IR-spectra of **II**, the H_3PO_4-bands at 3550, 1170 and 988 cm^{-1} are more intensive compared to **I**.

3.2 *Crystal structure*

The crystal structure of **I** is made up of complex cations *trans*-[Ru(NO)$Py_2Cl_2(H_2O)]^+$, outersphere $H_2PO_4^-$ anions and molecules of phosphoric acid and water. The structure of the complex with atomic numbering and thermal displacement ellipsoids is shown in Figure 1. Selected bond lengths and bond angles are listed in Table 2.

The pyridine molecules are *trans* to each other; the square environment in the equatorial plane is completed with two chloride ions. The Ru–N(Py) bond lengths are ∼2.1 Å. The RuCl bond lengths are ∼2.35 Å. The axial positions in complex **I** are occupied by the nitrosyl group and water molecule. The Ru–O(1) bond length is ∼2.05 Å. The geometrical parameters of the fragment $\{RuNO\}^{3+}$ also agree well with the literature data;[12,16,18] the NO and Ru–N(NO) bond lengths are nearly 1.15 and 1.72 Å, respectively; the O–N–Ru angle approximates to 180°. In the complex, the central Ru atom deviates from the equatorial plane by ∼0.1 Å toward the nitrosyl-group.

In the coordinated pyridine molecules, the average N–C and C–C bond lengths have standard values (∼1.35 and 1.38 Å, respectively). The planes of the

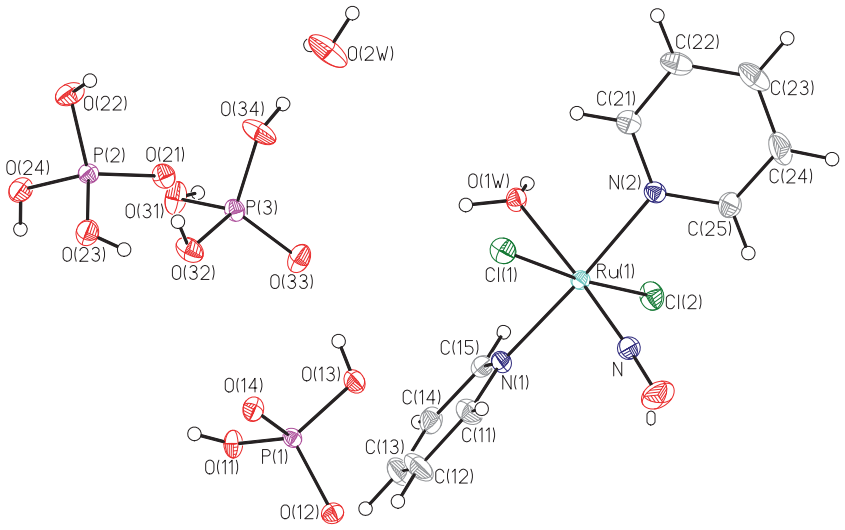

Figure 1. The structure of *trans*-$[Ru(NO)Py_2Cl_2(H_2O)]^+$ with outer-sphere environment in compound **I**. The coordination polyhedron of the Ru atom is a slightly distorted octahedron (RuN_3Cl_2O). The bond angles at the Ru atoms deviate from 90° by at most 5.8°.

Table 2. Selected bond lengths and bond angles in *trans*-$[Ru(NO)Py_2Cl_2(H_2O)]H_2PO_4{\cdot}2H_3PO_4{\cdot}H_2O$ (**I**).

Bond	*d*, Å	Bond	*d*, Å
N–O	1.150(2)	Ru–N(2)	2.0955(18)
Ru–N	1.7171(19)	Ru–Cl(1)	2.3560(6)
Ru–O(1)	2.0479(15)	Ru–Cl(2)	2.3521(6)
Ru–N(1)	2.1063(18)		
Angle	***ω*.°**	**Angle**	***ω*.°**
O–N–Ru	176.61(19)	N–Ru–Cl(2)	95.08(6)
N–Ru–O(1)	175.70(8)	O(1)–Ru–Cl(1)	84.26(5)
N–Ru–N(1)	91.30(8)	O(1)–Ru–Cl(2)	88.97(5)
N–Ru–N(2)	93.35(8)	N(1)–Ru–Cl(1)	90.51(5)
O(1)–Ru–N(1)	87.21(7)	N(1)–Ru–Cl(2)	90.72(5)
O(1)–Ru–N(2)	88.21(7)	N(2)–Ru–Cl(1)	90.14(5)
N(1)–Ru–N(2)	175.28(7)	N(2)–Ru–Cl(2)	88.08(5)
N–Ru–Cl(1)	91.72(6)	Cl(2)–Ru–Cl(1)	173.06(2)

pyridine rings make with each other angles of ~90°, the angles between their planes and the equatorial plane are 45–55°.

In the dihydrophosphate-ion the P–OH bond length is 1.56–1.57 Å; the other three P–O bonds are close in length to each other (on average, ~1.50–1.51 Å). The anions are united through the hydrogen bonds O–H···O (2.6 Å). The bond distances in H_3PO_4-molecules are about 0.01–0.02 Å shorter.

The general view of the packing pattern in the crystal of complex **I** is shown in Figure 2. The complex cations are linked to the dihydrophosphate ions by hydrogen bonds involving the coordinated water molecule and the O atoms of the $H_2PO_4^-$ (O(w)···O 2.5–2.9 Å). The shortest Ru...Ru distance is 6.0 Å. Half of pyridine-molecule is linked by π-stacking interaction with evaluated distance of C...C ~3.7 Å.

3.3 *TGA studies*

Compounds **I** and **II** were studied by thermal analysis (Figure 3). There are no clear-cut steps in thermal curves apart from the first step of thermolysis of **I** at ~90°C, when the compound loses one outer-sphere water molecule (calc. –2.7%, found on TG-curve –2.4%).

The thermal decomposition of **II** also starts by losing crystallization water molecule, but the corresponding process is not fixed apart at the TG curve, because there are two other processes of removal of water – decomposition of $H_2PO_4^-$ and aqua-complex. According to the previous studies of thermal properties of nitrosyl ruthenium pyridine complexes,[16] the heating of **I** and **II** at ~200°C must result in the loss of pyridine molecules. Further decomposition of **I** and **II** (above 300–350°C) occurs in several poorly resolved stages which are attributed to mixed processes of coordinated pyridine molecule decomposition, removal of NO and HCl.[16,19] The final products, as indicated by powder X-ray diffraction, contain nano-powder ruthenium phosphides RuP, Ru_2P and RuP_2.

The products of thermolysis of **I** (up to 780°C) are RuP (82±5% mass., OCD ~20 nm), Ru_2P (7±5% mass., OCD ~80 nm) and RuP_2 (11±5% mass.) (see Figure S1 and Table S1 in Supplementary Information). The average molar mass of the products of thermolysis

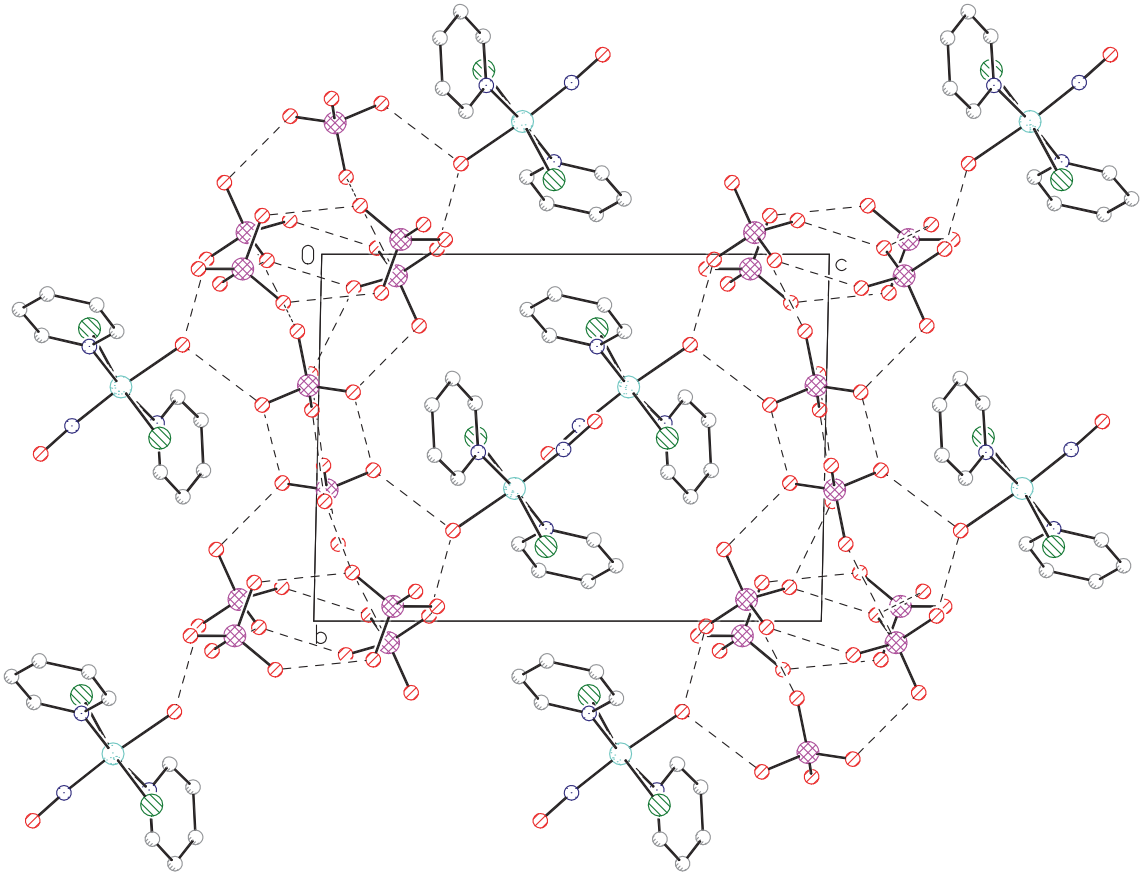

Figure 2. The general view of the packing pattern in the crystal of complex **I** along the *x*-axis.

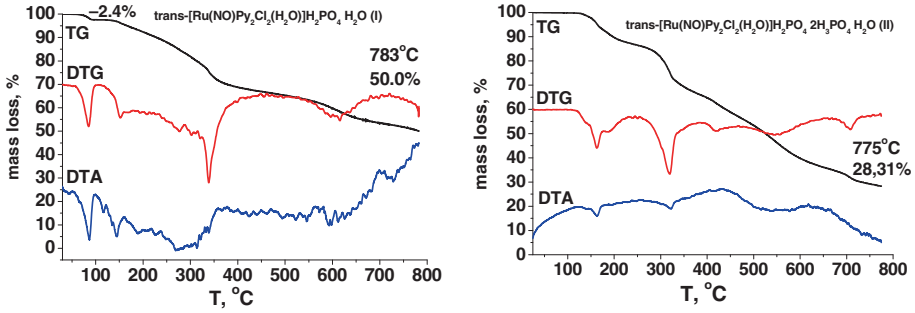

Figure 3. TGA-curves for **I** and **II** in He atmosphere.

of **I** is 336.8 a.m.u., which indicates that the sample contains other amorphous phase, as indicated by IR spectra – it is polyphosphate complexes of ruthenium (ω, cm^{-1}: 1100 sh s wide; 980 *vs* wide $\nu_{as}(PO_4)$; 492 s $\nu_s(PO_4)$; 401 sh m ν(Ru-O)). The products of thermolysis of **II** (up to 780°C) are RuP (~90±5% mass., OCD ~30 nm) and Ru_2P (10±5% mass., OCD ~80 nm) (see Figure S2 and Table S2 in Supplementary Information). The average molar mass of the products of **II** is 135,1 a.m.u., which indicates that the sample contains a small amount (~3 a.m.u.) of amorphous CHN-phase. The nitric acid solution of thermolysis product analysed by ICPMS method, found that the product contains 19.8% of phosphorous (calculated 20.7%); the ruthenium content was much lower than the calculated value (Found 11.3% of ruthenium, calculated 79.3%), probably due to bad resolution of Ru for this analytical method.

The investigation by scanning electron microscopy confirms the dimensions of nanoparticles. Microphotograph of thermolysis products of **I**, obtained by detector of backscattered electrons, shows three phases: light, medium and hard (Figure S3a). The microphotographs obtained by both detectors – secondary and backscattered electrons show that harder particles of thermolysis

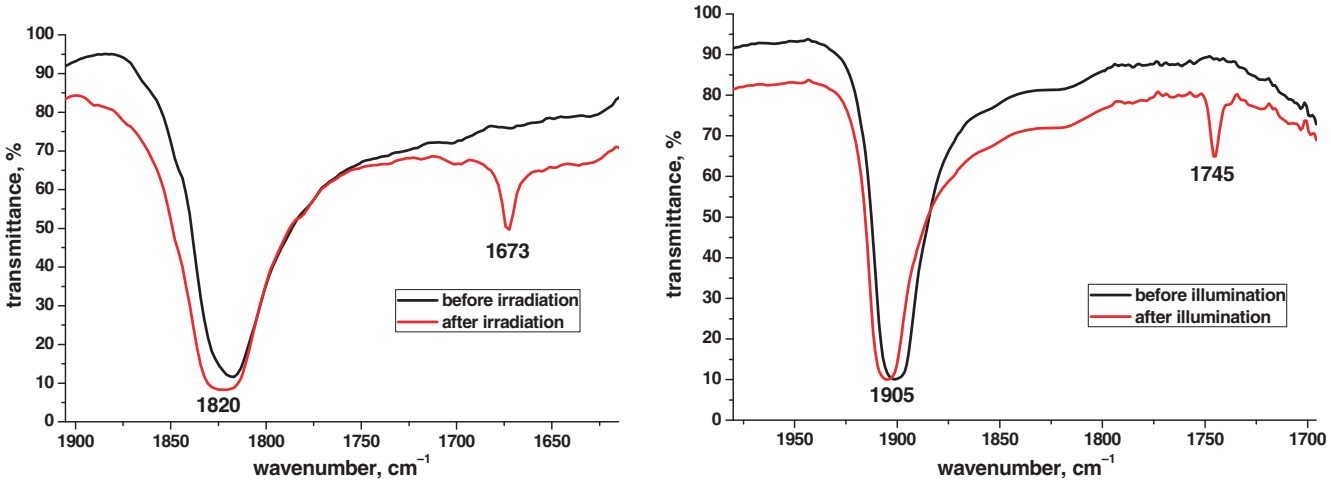

Figure 4. Infrared spectra of *trans*-[Ru(NO)$Py_2Cl_2(OH)$] (left) and **II** (right) in the spectral region of the ν(NO) stretching vibration in the ground state (GS) and after illumination.

product **II** are covered by lighter substance, which is practically invisible in backscattered electron image (Figure S3b, c).

3.4 *Photoisomerization studies*

The photochemical transformations that occurred under the illumination of the polycrystalline samples of compounds, *trans*-[Ru(NO)$Py_2Cl_2(OH)$] and *trans*-[Ru(NO)$Py_2Cl_2(H_2O)$]$H_2PO_4 \cdot H_2O$ (**II**) were studied by IR spectroscopy. An additional band at 1673 cm^{-1} (for *trans*-[Ru(NO)$Py_2Cl_2(OH)$]) and 1745 cm^{-1} (for **II**), which can be interpreted as ν(NO) for the MS1 state,[10,11] appears in the IR spectrum of the irradiated sample (Figure 4). The difference between ν(NO) signals for ground state (GS) and metatstable state (MS1) is about 150 cm^{-1} (for *trans*-[Ru(NO)$Py_2Cl_2(OH)$]) and 160 cm^{-1} (for aqua complex **II**) which are slightly higher that corresponding difference for other nitrosyl pyridine complexes of ruthenium: ~130 cm^{-1} (for *cis*-[Ru(NO)$Py_2(NO_2)_2(OH)$][11]), ~140 cm^{-1} (for *cis*-[Ru(NO)$Py_2Cl_2(OH)$][20] and *fac*-[Ru(NO)Py_2Cl_3][21]).

The DSC method was used to study the kinetics of the backward isomerization of the MS1 state. The measurements were carried out for three different weighed samples at different heating rates. The resulted dependence of the heat flow on temperature (Figure 5) is well approximated by the first-order kinetics[20]:

$$\dot{H} = H_{tot} \cdot k_0 \cdot \exp\left(-\frac{E_a}{k_B \cdot T} - \frac{k_0}{q}\int_{T_0}^{T} e^{-\frac{E_a}{k_B \cdot T'}} \cdot dT'\right),$$

Where, $\dot{H}$ is the heat flow, H_{tot} – the overall effect, k_0 – the pre-exponential factor, E_a – activation energy, q – ramp rate, k_B – the Boltzmann constant, T_0 – the starting temperature.

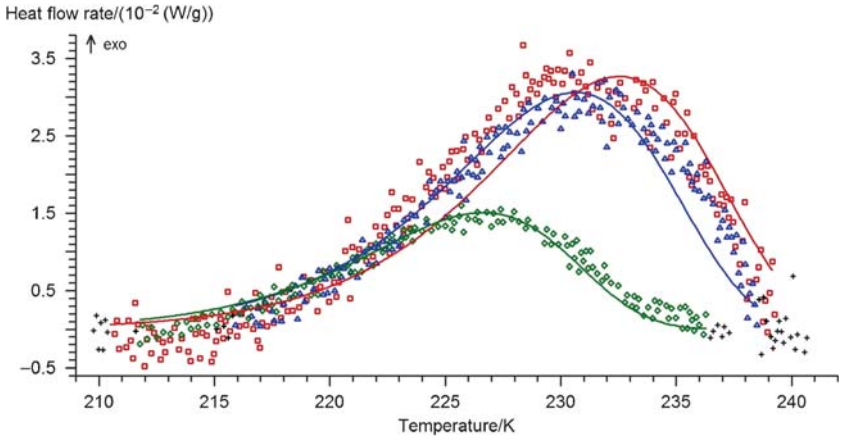

Figure 5. Calculated (lines) and experimental (dots) DSC curves for *trans*-[Ru(NO)$Py_2Cl_2(H_2O)$]$H_2PO_4 \cdot H_2O$ (**II**) (green – 3 K/min, red – 6K/min and blue –9 K/min).

All the curves were calculated in a range of 209–241 K giving E_a and $\log_{10}(k_0/\text{sec}^{-1})$ as 90.7±2.4 kJ/mol and 18.9±0.6, respectively. It was suggested earlier[22] that the decomposition temperature (T_d) of MS1 can be accepted as the value corresponding to the decay rate of 10^{-3} s^{-1}. For the studied compound, $T_d = 217$ K.

The DSC experiment for *trans*-[Ru(NO)Py_2Cl_2(OH)] was uninformative, because the yield of MS1-isomer was so small and hence the thermal effect is almost invisible (see Figure S4 in Supplementary Inforamtion).

4. Conclusions

We have prepared *trans*-[Ru(NO)$Py_2Cl_2(H_2O)$]$H_2PO_4\cdot 2H_3PO_4\cdot H_2O$ (**I**) and *trans*-[Ru(NO)$Py_2Cl_2(H_2O)$]$H_2PO_4\cdot H_2O$ (**II**) in high yields. Compound **I** has been structurally characterized by XRD, and the calculated diffractogram corresponds to powder diffraction data. Both compounds have been characterized by thermal analysis. Heating of salts up to ∼780°C affords a mixture of ruthenium phosphides. Thus, RuP (∼80% mass) with admixtures of Ru_2P and RuP_2 in amorphous polyphosphate ruthenium phase from **I** and RuP (∼90% mass) with impurity of Ru_2P from **II**, were inferred by powder X-ray diffraction, ICP-MS analysis and electronic microphotography. Preliminary photoisomerization experiments on *trans*-[Ru(NO)Py_2Cl_2(OH)] and *trans*-[Ru(NO)$Py_2Cl_2(H_2O)$]$H_2PO_4\cdot H_2O$ (**II**) were performed, and metastable states were indicated by IR spectroscopy with stretching bands (NO) at 1673 cm^{-1} (*trans*-[Ru(NO)Py_2Cl_2(OH)]) and 1745 cm^{-1} (**II**). DSC experiments have been carried out for both the compounds. The measured kinetic parameters of MS1 decay for *trans*-[Ru(NO)$Py_2Cl_2(H_2O)$]$H_2PO_4\cdot H_2O$ are E_a = 90.7±2.4 kJ/mol, $\log_{10}(k_0/\text{sec}^{-1})$ = 18.9±0.6, and T_d = 217 K.

Supplementary Information (SI)

CCDC No. 1476880 contains the supplementary crystallographic data for this paper. These data can be obtained free of charge from the Cambridge Crystallographic Data Centre *via* www.ccdc.cam.ac.uk/data_request/cif. DSC curve for *trans*-[Ru(NO)Py_2Cl_2(OH)], powder diffraction data and microphotographs for thermolysis products of **I** and **II** are available in Supplementary Information at www.ias.ac.in/chemsci.

Acknowledgements

Authors thank Dr. Gennady A. Kostin and Artem A. Mikhailov for laser experiments; Dr. Anna P. Zubareva, Dr. Olga S. Kosheeva and Dr. Alphiya R. Tsygankova for the elemental analysis; Dr. Dmitry P. Pischur for recording the DSC curves; and Natalya P. Korotkevich for powder X-ray diffraction study.

References

1. Teller H, Krichevski O, Gur M, Gedanken A and Schechter A 2015 Ruthenium Phosphide Synthesis and Electroactivity toward Oxygen Reduction in Acid Solutions *ACS Catal.* **5** 4260
2. Guan Q, Sun C, Li R and Li W 2011 The synthesis and investigation of ruthenium phosphide catalysts *Catal. Commun.* **14** 114
3. Kaner R, Castro C A, Gruska R P and Wold A 1977 Preparation and characterization of the platinum metal phosphides RuP_2 and IrP_2 *Mat. Res. Bull.* **12** 1143
4. Honle W, Kremer R and Schnering H G 1987 Ruthenium(III)triphosphide RuP_3: Preparation, crystal structure and properties *Z. Kristallogr.* **179** 443
5. Gopalakrishnan J, Pandey S and Rangan K K 1997 Convenient Route for the Synthesis of Transition-Metal Pnictides by Direct Reduction of Phosphate, Arsenate, and Antimonate Precursors *Chem. Mater.* **9** 2113
6. Schaniel D, Woike T, Delley B, Boskovic C, Biner D, Krämer K W and Güdel H U 2005 Long-lived light-induced metastable states in *trans*-[$Ru(NH_3)_4(H_2O)NO]Cl_3\cdot H_2O$ and related compounds *Phys. Chem. Chem. Phys.* **7** 1164
7. Kushch L A, Golhen S, Cador O, Yagubskii E B, Il'in M A, Schaniel D, Woike T and Ouahab L 2006 Photochromic Molecular Material Based on Anderson–Evans Polyoxometalate $[Cr(OH)_6Mo_6O_{18}]^{3-}$ and Ruthenium Mononitrosyl Complexes $[RuNO(NH_3)_4(X)]^{n+}$ (X = NH_3, OH; n = 3, 2) *J. Cluster Sci.* **17** 303
8. Schaniel D, Woike T, Kushch L and Yagubskii E 2007 Photoinduced nitrosyl linkage isomers in complexes based on the photochromic cation $[RuNO(NH_3)_5]^{3+}$ with the paramagnetic anion $[Cr(CN)_6]^{3-}$ and the diamagnetic anions $[Co(CN)_6]^{3-}$ and $[ZrF_6]^{2-}$ *Chem. Phys.* **340** 211
9. Rose M J and Mascharak P K 2008 Photoactive ruthenium nitrosyls: Effects of light and potential application as NO donors *Coord. Chem. Rev.* **252** 2093
10. Cormary B, Ladeira S, Jacob K, Lacroix P G, Woike T, Schaniel D and Malfant I 2012 Structural Influence on the Photochromic Response of a Series of Ruthenium Mononitrosyl Complexes *Inorg. Chem.* **51** 7492
11. Kostin G A, Borodin A O, Mikhailov A A, Kuratieva N V, Kolesov B A, Pishchur D P, Woike T and Schaniel D 2015 Photocrystallographic, Spectroscopic, and Calorimetric Analysis of Light-Induced Linkage NO Isomers in $[RuNO(NO_2)_2(pyridine)_2OH]$ *Eur. J. Inorg. Chem.* **29** 4905
12. Makhinya A N, Il'in M A, Kabin E V, Baidina I A, Gallyamov M R and Alferova N I 2014 Nitrosoruthenium hydroxo and aqua complexes of the trans-dipyridine series: Synthesis, structures, and characterization *Russ. J. Coord. Chem.* **40** 297

13. Emel'yanov V A, Fedotov M A, Belyaev A V and Tkachev S V 2013 A multinuclear magnetic resonance study of transformations of ruthenium(II) nitrosyl chloride complexes in aqueous solutions *Russ. J. Inorg. Chem.* **58** 956
14. Powder Diffraction File, release 2010, International Centre for Diffraction Data, Pennsylvania, USA
15. Sheldrick G M 2007 A short history of SHELX *Acta Crystallogr., Sect. A: Found. Crystal* **64** 112
16. Makhinya A N, Il'in M A, Baidina I A, Plyusnin P E and Gallyamov M R 2014 Structure and properties of tripyridine nitrosocomplexes of ruthenium: *Mer*-[Ru(NO)Py_3Cl(OH)]Cl1.5H_2O and *mer*-[Ru(NO)Py_3Cl(H_2O)]Cl_2·2H_2O0.5HCl *J. Struct. Chem.* **55** 682
17. Il'in M A, Emel'yanov V A, Baidina I A, Alferova N I and Korol'kov I V 2007 Study of nitrosation of hexaammineruthenium(II): Crystal structure of *trans*-[RuNO$(NH_3)_4$Cl]Cl_2 *Russ. J. Inorg. Chem.* **52** 62
18. Emel'yanov V A, Baidina I A, Il'in M A and Gromilov S A 2006 Synthesis and crystal structure of nitrosoruthenium aquadiammine complex, [Ru(NO)$(NH_3)_2Cl_2(H_2O)$]Cl· H_2O *J. Struct. Chem.* **47** 380
19. Makhinya A N, Il'in M A, Baidina I A, Plyusnin P E, Alferova N I and Pishchur D P 2014 Structure, synthesis, and thermal properties of *trans*-[Ru(NO)$(NH_3)_4(SO_4)$]NO_3·H_2O *J. Struct. Chem.* **55** 311
20. Makhinya A N, Il'in M A, Yamaletdinov R D, Korolkov I V and Baidina I A 2016 Synthesis and crystal structure of nitrosoruthenium complexes *cis*-[Ru(NO)Py_2Cl_2(OH)] and *cis*-[Ru(NO)$Py_2Cl_2(H_2O)$]Cl. Photoinduced transformations of *cis*-[Ru(NO)Py_2Cl_2(OH)] *New J. Chem.* **40** 10267
21. Makhinya A N, Il'in M A, Yamaletdinov R D, Baidina I A, Tkachev S V, Zubareva A P, Korol'kov I V and Piryazev D A 2016 Synthesis, some properties, and crystalline modifications of *fac*-[Ru(NO)$(Py)_2Cl_3$] *Russ. J. Coord. Chem.* **42** 768
22. Ookubo K, Morioka Y, Tomizawa H and Miki E 1996 Vibrational spectroscopic study of light-induced metastable states of ethylenediaminenitrosylruthenium(II) complexes *J. Mol. Struct.* **379** 241